

# Single Wire Quadrant : Horizontal Omni-Directional Short Wave Aerial Comparisons

## 1. Purpose

Describe a quasi-omni-directional, horizontally polarised, short wave aerial having two single wire arms in a horizontal 90° Vee quadrant configuration. Compare this with other omnidirectional and quasi-omnidirectional configurations

## 2. Background

In 1944, Wells<sup>1</sup> described a horizontal cage quadrant, quasi-omni-directional aerial, with two  $\lambda/2$  arms, for short waves. Wire cages were used for each of the  $\lambda/2$  radiating arms in order to lower the drive point impedance, since a single wire dipole or quadrant with  $\lambda/2$  arms has a very high drive point impedance, typically 5,000  $\Omega$  at resonance. A side benefit of this cage construction was the widened bandwidth associated with any radiator having a large diameter to length ratio. Typically a satisfactory pattern could be maintained and receive VSWR was acceptable, over an octave of bandwidth. At the extremities of the octave band some pattern degradation was apparent, while the 2 : 1 transmit VSWR bandwidth was typically 13 – 14 %. A disadvantage of this design was the high weight and wind loading associated with the multiple wires and spreaders required to construct the cage radiators. Three substantial masts, typically with 600 mm. faces were required to support the antenna. Rigging was complex, typically taking an experienced, well equipped rigging team at least 3 days for fabrication, erection and tensioning using a power driven winch. Typical implementation used four masts arranged in a square to support four quadrant antennas that together covered the entire shortwave band. Implementation of this otherwise promising design appears beyond the resources of the average radio amateur on a suburban block.

As noted by Tai<sup>2</sup> an omnidirectional pattern is obtained when the limbs of the quadrant are of the order of  $\lambda/2$  long. Wells did note the possibility of a single  $\lambda/2$  wire for each of the radiating arms but did not pursue the idea further as the drive point impedance, for a V-quadrant with total length =  $\lambda$ , became high, with narrow bandwidth, making it unsuited to the application envisaged by Wells.

A single wire radiator construction is attractive for amateur use. Lighter weight and lowered wind loading allow use of lighter masts, or even fortuitously positioned trees, as support structures.

Everitt and Byrne<sup>3</sup> described, among many antenna configurations, methods of using a single wire transmission line driven against ground, with a critically positioned tap, for excitation of a half wavelength long horizontal wire radiator. This particular configuration appeared to be popular in the U.K. as the "Windom Aerial". Of particular interest is the two radiator broadside array known as the balanced windom<sup>4</sup>. This comprises two  $\lambda/2$  tapped radiators in colinear broadside array configuration, with the tap feeders in antiphase or push-pull, brought together in a delta configuration, to provide a 600  $\Omega$  balanced feed. This minimises feeder radiation, eliminates the requirement for an earth connection with its attendant losses, and allows use of readily constructed, low loss, 600  $\Omega$  open wire line. Configuration is similar to a delta matched half-wave dipole, but with a total length one wavelength and an open circuit or 'cut' at the midpoint. The 'cut' is necessary since the adjacent ends of the two half-wave radiators are at opposite potentials at a current zero.

## 3. Single Wire Quadrant

If the radiating  $\lambda/2$  elements are changed from a horizontal colinear configuration to a 90° quadrant configuration, with the radiating elements both still contained in a horizontal plane, with the tap points adjusted to provide the requisite drive point impedance, then the configuration now becomes a single wire quadrant antenna. Azimuth radiation pattern now becomes quasi-omnidirectional. Tap points can be selected to match various convenient impedances of open wire or

<sup>1</sup> Wells, N. "The Quadrant Aerial : an Omni-Directional Wide Band Horizontal Aerial for Short Waves" Journal of I.E.E. (London) part III, vol. 91, December 1944, pp. 182-193.

<sup>2</sup> Tai, C. T. , in Jasik, H. editor "Antenna Engineering Handbook" 1st. ed. McGraw-Hill 1961, ch. 3 pp. 3-26

<sup>3</sup> Everitt, W.L. & Byrne, J.F. "Single Wire Transmission Lines for Short Wave Antennas" Proc. I.R.E. v.17 no. 10, October 1929, pp. 1840-67

<sup>4</sup> Radio Society of Great Britain "Amateur Radio Handbook" 3rd. ed. 1961, ch. 3, pp. 362-3.

balanced line. Any required balun transformer can now be pole mounted near ground level to avoid the requirement to suspend the balun transformer weight aloft.

This configuration could be described as a "balanced double windom quadrant antenna", or as a "cut-delta single wire quadrant" based on its superficial similarity to a delta matched dipole with a lengthened horizontal and bent into a quadrant, but with a "cut" or insulating section, in the centre of the bent horizontal portion of the delta. First description is a trifle verbose, the second not much better, although somewhat more descriptive of the physical configuration.

First implementation for proof-of-concept was summer 1994-5 on the 52 MHz amateur band using three conveniently placed trees in the back garden. Initial band choice was prompted by presence of suitable materials in the "junk box" and ease of rigging using a step-ladder. Next trial was on the 15 metre amateur band at the same location. Subsequently, in 1997 the idea was conveyed to colleagues : a number of cut-delta quadrants were designed and placed in successful commercial service. Choice of the design was based on low cost and requirement for only a single frequency of operation.

#### 4. Cut Delta Quadrant Patterns

Figure 1 is for a single wire cut-delta quadrant resonant at 7.15 MHz, suspended at  $5\lambda/12$  height above average ground of conductivity 10 mS/metre, dielectric constant 13. Maximum gain is 5.4 dBi : variation  $\pm 0.9$  dB for varying azimuth at 35° elevation. Suspension height is somewhat ambitious for an amateur installation on the 40 metre band : it was chosen to illustrate the possibilities for a quasi-omnidirectional antenna suspended at a height to yield approximately constant field strength, independent of distance, for signals out to about 1500 km, i.e. a single ionospheric hop.

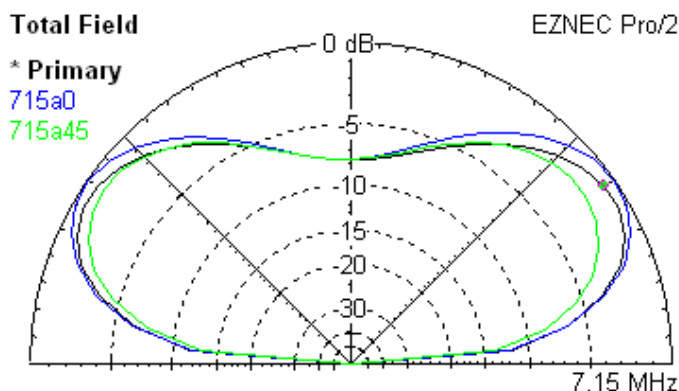


Fig 1 : Elevation patterns 5λ/12 height : 0°, 45°, 90° azimuth

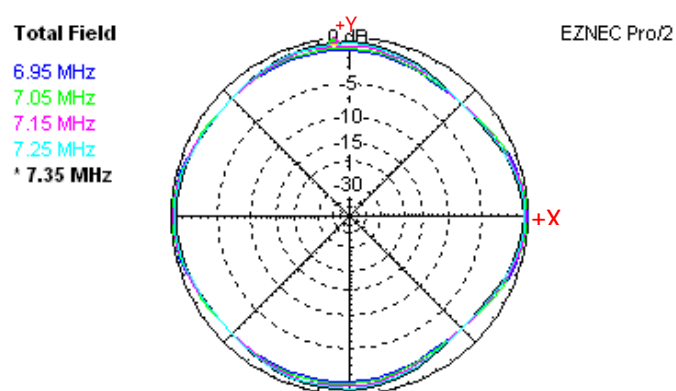


Fig 2 : Azimuth Patterns @ 35° elevation, 5.4 dBi gain

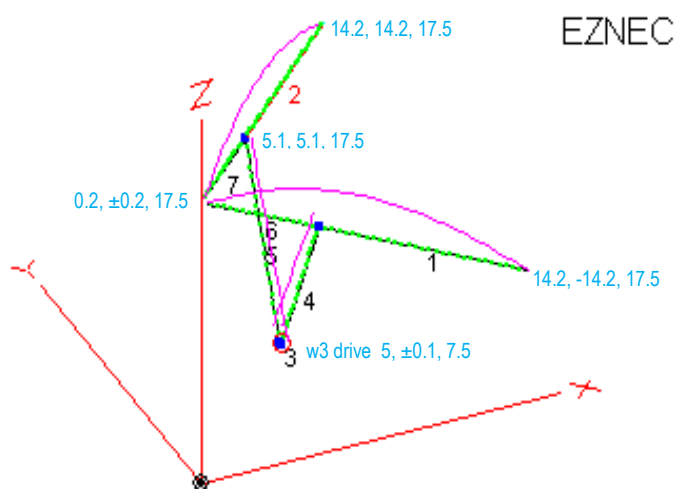


Fig 3 : Antenna Layout 3-D Co-Ordinates

MHz	Impedance : $\Omega$	VSWR : 600 $\Omega$
6.9	669 - j 453	2.03
7.0	630 - j 274	1.56
7.1	610 - j 94	1.17
7.15	606 - j 3	1.01
7.2	608 + j 91	1.16
7.3	624 + j 290	1.60
7.4	664 + j 509	2.21

Table 1 : Antenna Impedance vs. Frequency

Figure 2 shows the azimuth pattern at 35° elevation, the beam maximum, as frequency is varied. Figure 3 shows a scaled 3-D view of the antenna superimposed on the reference co-ordinates. Wires are shown in green, numbered in black, with current magnitudes in purple, end coordinates rounded to 0.1 m. in blue. Note the near-constant currents on the feeder sections of the delta, while the current magnitudes on the horizontal radiating sections have near equality each side of the tap points. This was the optimum adjustment criterion used by Everitt and Byrne<sup>3</sup> in 1929 for a single horizontal radiator fed by a vertical single wire transmission line. Table 1 records the impedances and VSWR calculated by EZNEC™, a commercial implementation of Numeric Electromagnetic Code, over the frequency band of interest.

Wire #	connect	Coordinates End 1: metres			connect	Coordinates End 2 metres			Dia.mm	Segments
		X	Y	Z		X	Y	Z		
1		14.185	-14.185	17.495	W4E1	5.1	-5.1	17.495	2.8	30
2		14.185	14.185	17.495	W5E1	5.1	5.1	17.495	2.8	30
3	W4E2	5.034	-.097	7.470	W5E2	5.034	.097	7.470	2.8	1
4	W6E1	5.1	-5.1	17.495	W3E1	5.034	-.097	7.470	2.8	21
5	W7E1	5.1	5.1	17.495	W3E2	5.034	.097	7.470	2.8	21
6	W1E2	5.1	-5.1	17.495		.208	-.208	17.495	2.8	18
7	W2E2	5.1	5.1	17.495		.208	.208	17.495	2.8	18

Table 2 : Wire Co-Ordinates in metres for the Cut-Delta Quadrant at 5 $\lambda$ /12 Height.

Table 2 documents the dimensions of the antenna and other parameters used in the calculation. Wire 3 is the drive point. Calculations are somewhat idealised : a real antenna will require slight adjustments to dimensions. This is not attributed to any shortcoming in the Numeric Electromagnetic Code. A real antenna will have end effects due to insulators, wire sag as tension is not infinite, diameter changes at crimps, abrupt change of slope at the tap points, impedance changes attributable to encroaching objects including support masts, guys, support catenaries, and impedance effects attributable to ground constants. If all effects taken into account in a detailed NEC model, it has been found practicable to calculate dimensions to an accuracy of  $\pm 5$  mm : extensive prior testing and experiment is required however.

### 5. Mounting Height Effects

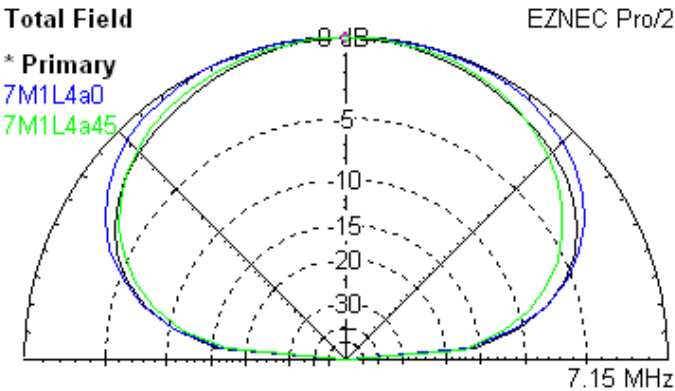


Fig 4 : Antenna  $\lambda$ /4 Height : Max Gain = 5.5 dBi @ 90°

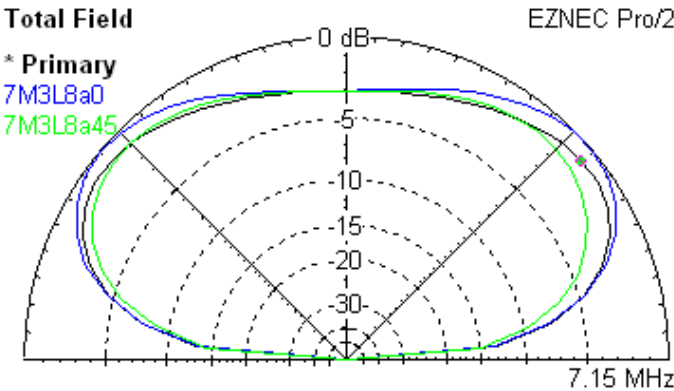


Fig 5 : Antenna  $3\lambda$ /8 Height : Max Gain = 4.3 dBi @ 40°

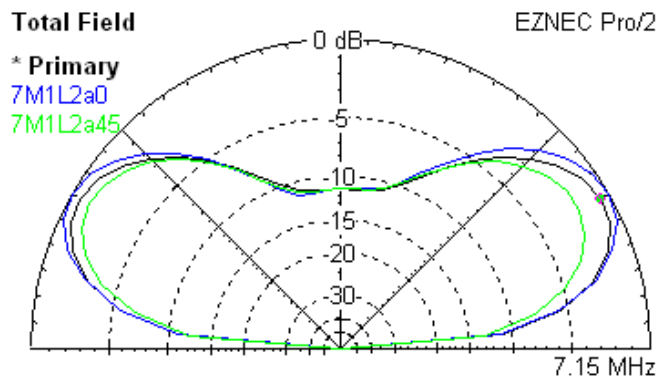


Fig 6 : Antenna  $\lambda/2$  Height : Max Gain = 5.8 dBi @ 30°

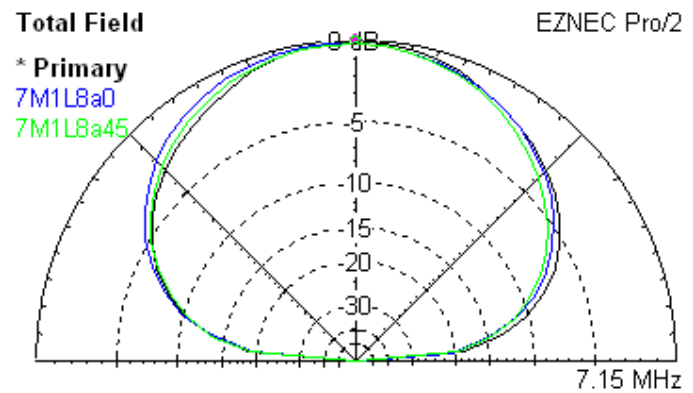


Fig 7 : Antenna  $\lambda/8$  Height : Max Gain = 5.2 dBi @ 90°

Figure 4, with the antenna at  $\lambda/4$  height, maximum gain 5.5 dBi is towards the zenith, gain  $\approx 0$  dBi at 20° takeoff angle. Figure 5, with the antenna at  $3\lambda/8$  height, maximum gain = 4.3 dBi at 40° takeoff angle, gain  $\approx 0$  dBi at 13 - 15° takeoff. Figure 6, with the antenna at  $\lambda/2$  height, maximum gain = 5.8 dBi at 30° takeoff angle, gain  $\approx 0$  dBi at 10° takeoff angle. Figure 7, with the antenna at  $\lambda/8$  height, maximum gain = 5.2 dBi towards the zenith, gain  $\approx 0$  dBi at 35° takeoff angle. Blue plots are for 0° azimuth, in the X-Z plane of symmetry. Green plots are 45° azimuth, in line with one of the arms of the quadrant. Black plots are 90° azimuth, at right angles to the line of symmetry bisecting the quadrant arms.

In each case arm length and tap points were adjusted to provide 600  $\Omega$  drive point impedance, VSWR  $\leq 1.02$  @7.15 MHz. Table 3 records the altered X and Y coordinates for Wire 2 End1 (outer end of radiating horizontal), Wire 5 End 1 (tap point of W5E1 between W2E2 and W7E1), and the altered X and Z coordinates for Wire 3 End 1. All other coördinates can be deduced by noting that the antenna is symmetrical about the X – Z plane, i.e. negative Y coordinates are mirror images of positive Y coordinates in this plane.

For the  $\lambda/4$  antenna the drive point was only 0.4 metre above ground level, a somewhat dangerous location. This could be avoided by changing the X-coordinate of the drive point of wire 3, i.e. moving the base of the delta match either away from, or towards, the apex of the quadrant to place the drive point at a somewhat safer height of 2 metres. Two options placing the drive point at 2 metres height are given for  $\lambda/4$  suspension. For the case of  $\lambda/8$  height this move was taken to an extreme : X-coordinate was 14.6 metres for both ends of wire 3. This preserved the length of the delta match feeders, was probably not optimum for bandwidth, but a provided a good match at 7.15 MHz.

Antenna Height	W2E1 : X & Y coord	W5E1: X & Ycoord.	W3E1 : X-coord.	W3E1 : Z-coord
$5\lambda/12 = 17.5$ m.	14.185	5.1	5.034	7.47
$\lambda/4 = 10.43$	14.04	5.08	5.034	0.4
$\lambda/4$	14.00	4.85	10.32	2.0
$\lambda/4$	14.07	5.4	0.5	2.0
$3\lambda/8 = 15.0$	14.14	5.03	5.034	4.97
$\lambda/2 = 20.0$	14.20	5.18	5.034	9.97
$\lambda/8 = 5.1$	14.08	5.2	14.6	2.0

Table 3 : Adjustments for Differing Antenna Heights

Suspension height of  $\lambda/4$  possibly represents a typical height for amateur use at 7MHz, while  $\lambda/8$  might be used where severe height restrictions apply. Heights of  $3\lambda/8$  and  $5\lambda/12$  might be useful on 14MHz with appropriate scaling of wire dimensions, while  $\lambda/2$  with very little high angle radiation but good low angle radiation would be appropriate at 21MHz. Above 20 MHz, stacked cage quadrants at  $\lambda/2$  and  $\lambda$  height, driven in phase, can completely suppress the useless high angle radiation while producing very low takeoff angles with +9 to +10 dBi gain and wide bandwidth. Stacked cages are somewhat ambitious for amateur use.

From Table 3 it is apparent that, after selecting the mounting height, the cut-delta quadrant has three principal degrees of freedom for fine adjustment. Overall length of the horizontal sections principally determines the resonant frequency. Movement of the tapping point is used to adjust impedance at resonance. Movement towards the "cut" lowers impedance. Lengthening the sloping wires of the delta raises impedances above resonance whilst simultaneously lowering impedances below resonance. All adjustments produce some interaction, so experimentation, measurement and repeated adjustments may be necessary for a completely satisfactory result.

## 6. Altered Drive Point Impedances

Table 4 shows the effects, on a  $\lambda/4$  mounting height antenna, of moving the tap point on the horizontal arms. The 600  $\Omega$  entry for reference comparison is the same as Table 3 with the W3 drive point  $X = 0.5$ ,  $Z = 2$  metres for all entries. Note that for 70  $\Omega$  and 50  $\Omega$  where W3  $X = 5.8$  in order to bring the length of matching feeder close to  $\lambda/4$  as the tap points have moved to the extreme inner position at the 'cut' point. For a 50  $\Omega$  match the wire spacing of the  $\lambda/4$  match section has been decreased to 110 mm.

Impedance	W2E1: X & Y coord.	W5E1: X & Y coord.	VSWR $\leq 2$ Bandwidth
600	14.07	5.4	6.91 – 7.38
450	14.14	5.08	6.93 – 7.35
300	14.30	4.56	6.95 – 7.35
200	14.59	3.97	6.97 - 7.32
70	W2E1= 14.7 W5E1 = 0.208 W3Xcoords. = 5.8		6.99 – 7.30
50	W2E1= 14.02 W5E1 = 0.055 W3Xcoords = 5.8		7.01 – 7.3

Table 4 : Modifications for Different Drive Point Impedances

Moving the tap point towards the 'cut' has the effect of lowering the drive point impedance. This may seem counter-intuitive as the 'cut' point is itself the point of highest impedance ( $\approx 5,000 \Omega$  at resonance). However the sloping wires of the delta match are behaving as an approximately  $\lambda/4$  transmission line to provide an impedance inversion between the tap points and the drive point. The sloping arms of the delta constitute a transmission line with a linear physical taper while the characteristic impedance changes in proportion to the logarithm of the wire spacing. Thus for the 600  $\Omega$  drive point impedance match the base of the line has a characteristic impedance  $\approx 600 \Omega$ , while at the tap points the characteristic impedance has risen to approximately 1,070  $\Omega$ . For the 200  $\Omega$  drive point impedance the line characteristic impedances are 600  $\Omega$  at base, 1,030  $\Omega$  at the tap. For 70  $\Omega$  drive point impedance the line characteristic impedance is 600  $\Omega$  at base, 680  $\Omega$  at the connections to the horizontal radiators at the 'cut' point. Thus the 70  $\Omega$  drive point impedance represents the extreme limiting case for matching using a  $\lambda/4$  impedance inverting line with characteristic impedance  $\approx 640 \Omega$ . To further lower the drive point impedance would require a  $\lambda/4$  line with a lower characteristic impedance. This is the technique for the 50  $\Omega$  match : impedance for the  $\lambda/4$  matching line has been lowered to 525  $\Omega$ . As the ratio between the

impedance at resonance for the quadrant alone and the impedance at the matching drive point becomes more extreme then the overall bandwidth decreases.

## 7. Stub Match

A short circuited  $\approx \lambda/4$  line may be connected to the quadrant 'cut' points and tapped at a suitable distance from the short for attachment to a balun or open wire line. This has the advantage that the short circuited end may be grounded as a static drain for lightning protection. A typical set of dimensions for a 600  $\Omega$  drive point might be : W2E1 X & y coords = 14.23, W2E2 x & y coords = 0.2, W2 height = 10.8 : W3 drive point x & y coords = 0.2, z coord. = 2.42 : W8 shorted end x & y coords = 0.2, z coord = 0.3

At 600  $\Omega$  impedance, VSWR < 2 over the range 6.99 – 7.32 MHz. This is less bandwidth than the simple cut-delta match. As the tap point is moved towards the shorted end of the  $\lambda/4$  matching line, the drive point impedance is lowered along with the bandwidth, so the technique has limitations.

This configuration is a variant on the streamlined "horizontal-U" quasi-omnidirectional antenna used on aircraft at VHF for localiser reception in early glide path guidance (blind landing) systems<sup>5</sup>.

## 8. Two $\lambda/2$ Dipoles in Quadrant Configuration.

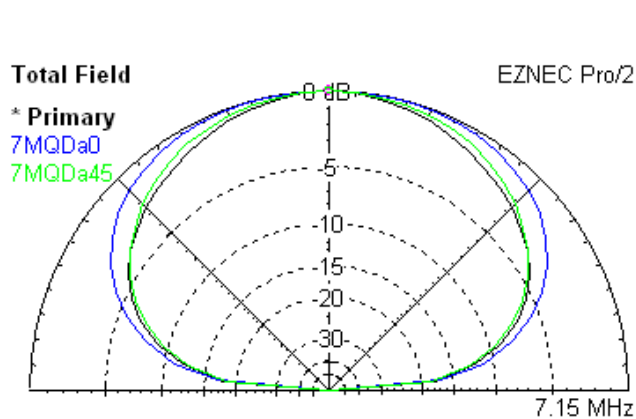


Fig 8 : Two  $\lambda/2$  dipoles in Quadrant : Elevation Patterns

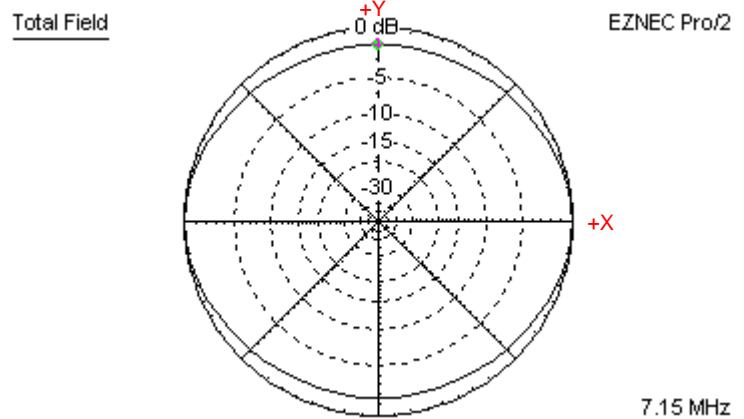


Fig 9: Quadrant  $\lambda/2$  dipoles Azimuth @ 45° elevn.  $\pm 0.8$  dB

If two horizontal  $\lambda/2$  dipoles at a height of  $\lambda/4$  are arranged in quadrant configuration and phased such that the adjacent ends at the apex of the quadrant are insulated from each other, and are in antiphase, ie. driven as though the two dipoles were part of a broadside array that has been bent into a quadrant, then the expected quasi-omnidirectional azimuth pattern is produced. Maximum deviation from omnidirectionality is  $\pm 0.8$  dB at 45° elevation angle. Drive point impedances are 86  $\Omega$  at resonance for each dipole, if centre driven, with a bandwidth of 6.89 – 7.45 MHz for VSWR  $\leq 2$ .

Moving the drive point for each dipole from the centre to a point 37% of the dipole length from the adjacent ends changes the drive point impedances at resonance to  $\approx 100$   $\Omega$  for VSWR  $\leq 2$  over the band 6.88 – 7.46 MHz. Virtually the same drive point impedance is achieved if the drive points are 63% from the adjacent ends, i.e. 37% from the remote ends. This opens up a number of possibilities for matching. Two matched length 50  $\Omega$  coaxial cables with their braids bonded and centre conductors driven in push-pull or antiphase will yield a balanced 100  $\Omega$  transmission line. With 100  $\Omega$  lines of matched length to feed each dipole, the remote ends can be brought together in the correct phase to provide a balanced 50  $\Omega$  feed point. This can then be converted to an unbalanced feed : one balun implementation is a simple Guanella balun

<sup>5</sup> Montgomery, B.E. "A Very-High-Frequency Aircraft Antenna for the Reception of 109-Megacycle Localizer Signals" Proc. IRE, v33 no.11 November 1945, pp. 767 - 772

made by threading multiple turns of a coaxial cable through a toroidal magnetic core. A static drain is advisable. Presence of the coaxial braids does result in a slight change of resonant frequency, but this can be compensated by a change in the length of the radiating arms. Figures 8 and 9 show the radiation patterns, figure 10 shows the configuration.

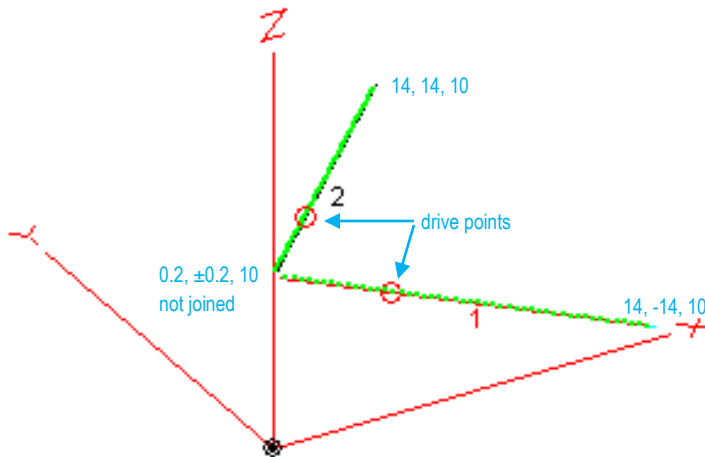


Fig 10 :Two  $\lambda/2$  Dipoles in Quadrant Configuration 3-D View

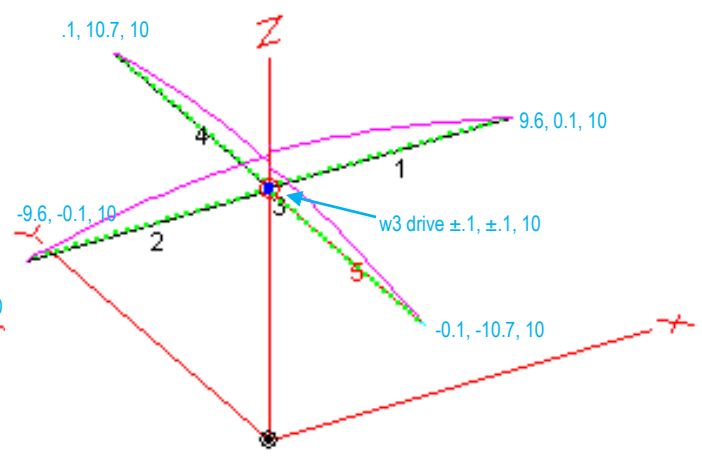


Fig 11 : Turnstile Arm Lengths Adjusted for Quadrature

## 9. Turnstile Antenna

Two horizontal, centre fed,  $\lambda/2$  dipoles may be mounted with their wire axes at right angles and drive points at near coincidence. I.e. drive points have the same X and Y coordinates but may differ very slightly in the Z coordinate. When the drive point currents are equal in magnitude but differ in phase by  $90^\circ$  the radiation pattern is very nearly omnidirectional in azimuth. Commonly this is referred to as a turnstile array. It has been used for VHF low band television transmission<sup>6</sup>. Another variant has been vertical log-periodic twin curtain arrays in a turnstile arrangement for wideband omnidirectional coverage : extensively used commercially, but highly ambitious for an amateur installation.

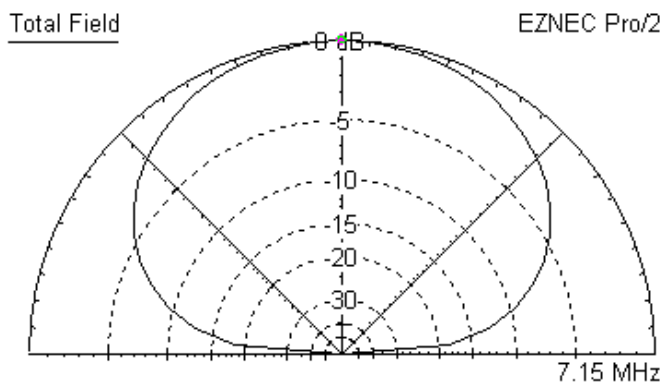


Fig 12 : Turnstile Array @  $\lambda/4$  height : gain = 6.2 dBi

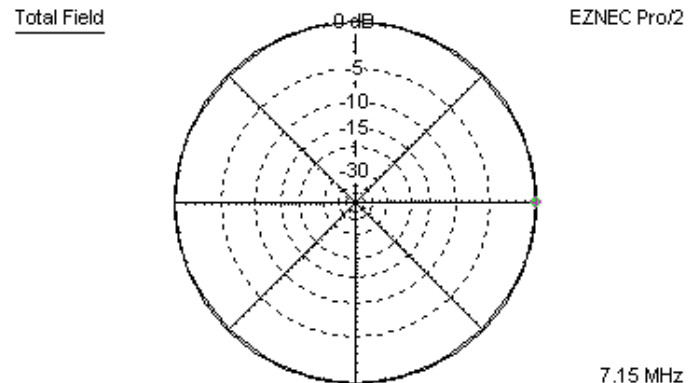


Fig 13: Turnstile Array Azimuth  $45^\circ$  Elvn. 4 dBi gain

Figures 12 and 13 show the elevation and azimuth patterns for a turnstile antenna mounted at a height of  $\lambda/4$  over average ground. Ominidirectionality is excellent. Obvious major disadvantages for shortwave use are the possible requirements for 4 support towers and for two balun transformers supported aloft. Drive point impedances are approximately  $70 - 80 \Omega$

<sup>6</sup> see for example : Terman F.E. "Radio Engineers' Handbook" McGraw-Hill 1943, pp. 870-1 or Lindenblad N.E. "Television Transmitting Antennas for Empire State Building" RCA Review, v3 april 1939, pp 387



balanced. A more subtle problem occurs with the phasing of the two dipoles : if located near the equator the sense of the 90° phase difference is not particularly critical. If located south of the equator then, when viewed from above, and moving counter-clockwise from a reference arm, excitation phase should lag by progressive 90° increments. In the northern hemisphere the phase sequence should be reversed. Reason for this arrangement is that the high angle radiation is circularly polarised. For the sense given, the circular polarisation should excite the 'Ordinary' wave in preference to the 'eXtraordinary' wave. The 'O' wave suffers significantly less attenuation when returned from the ionosphere, while the 'X' wave has a measurably higher MUF. Both of these effects result from interaction of the propagating wave with electrons in the ionosphere in the presence of the vertical component of the earth's magnetic field. Since the direction of the vertical component of the earth's magnetic field is different for the two hemispheres the optimum sense of circular polarisation reverses. As a generalisation, the turnstile does not appear to be an optimum choice for an inexpensive, compact, shortwave, amateur installation.

Usually the 90° phase difference is produced by use of an  $\lambda/4$  transmission line but an alternative is to make one dipole shorter, i.e. slightly below resonance at the operating frequency, the other longer, to make it above  $\lambda/2$  resonance at the operating frequency as shown in figure 11. Another alternative is to load one dipole with two series capacitors, the other with two series inductors at the drive points to obtain the required 90° phase difference. Both of these latter approaches have the advantage that a common drive point can now be used for the crossed dipoles. Table 5 compares results for the three different methods : in each case the bandwidth is increased compared to the simple cut delta quadrant since the reactance changes for the two dipoles tend to cancel in the region of dipole resonance. Compare this with the cut-delta match, where shortening one arm and lengthening the other does not improve bandwidth.

Configuration	Achieved by	40 $\Omega$ VSWR $\leq 2$	50 $\Omega$ VSWR $\leq 2$	70 $\Omega$ VSWR $\leq 2$
$\lambda/4$ line	10 metres of 80 $\Omega$ air line equivalent	6.65 – 7.8 MHz	6.7 – 7.7 MHz	
short/lengthen	X = - 4% , Y = + 7%		6.6 – 7.6 MHz	6.55 – 7.7 MHz
loading	X = 2 x 600 pF, Y = 2 x 1 $\mu$ H series		6.65 – 7.5 MHz	6.7 – 7.65 MHz
Tstl. 0° shift	X&Y arms: -X&-Y arms commoned	6.86 – 7.37 MHz	6.86 – 7.4 MHz	
Inv-V Tstl. 0°	X&Y arms: -X&-Y arms commoned	7.0 – 7.33 (25 $\Omega$ )	7.1 – 7.3 MHz	

Table 5 : Comparison of Turnstile Phasing Arrangements

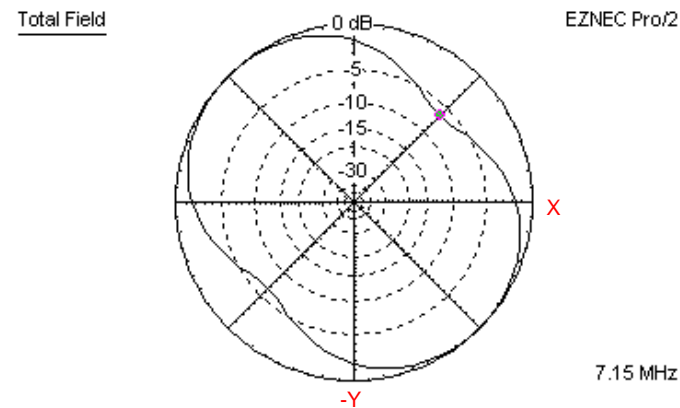


Fig 14 : Turnstile : no phase shift Azimuth @ 30° Elevatio

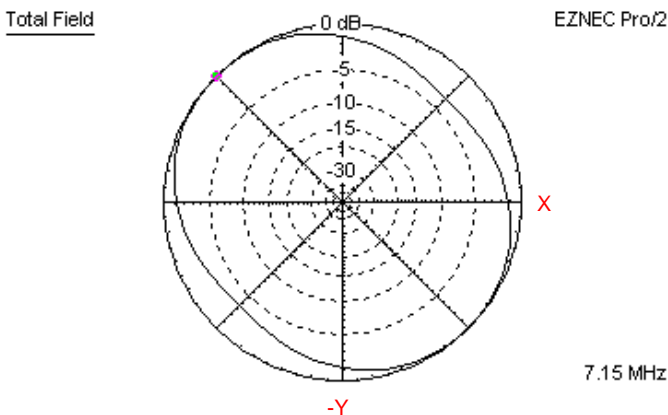


Fig 15 : Invrtd-V Turnstl. no phase shift @ 30° Elevn.



Figures 14 and 15 have been included for comparison purposes<sup>7</sup>. Figure 14 is for the turnstile array of fig. 11, but with the arm lengths made equal such that the progressive 90° phase difference between adjacent arms is not present : drive is between X&Y joined arms and -X&-Y joined arms. Pattern difference between maximum and minimum at 30 deg elevation is 6.4 dB. Fig 15 is for the the inverted vee turnstile of fig. 27, but with all arm lengths equal in length : i.e. lacking the 90° phasing. Pattern difference is 3.7 dB. Pattern differences increase as elevation angle reduces.

## 10. Simple Horizontal $\lambda/2$ Dipole

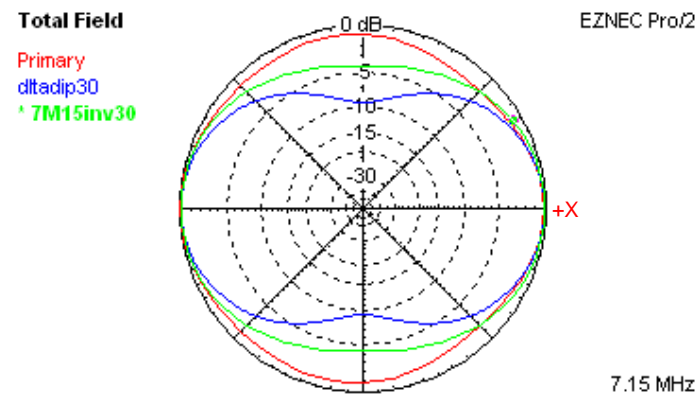


Fig 16: Patterns for Quad, Horz. Dipole, Inverted Vee

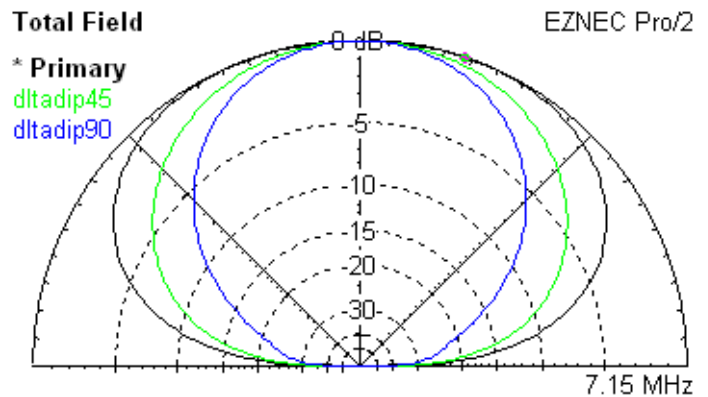


Fig 17 : Pattern for Horz. Dipole @ 0°, 45°, 90° azimuths

Figure 16 compares the azimuth patterns at 30° elevation for a simple, symmetrically driven,  $\lambda/2$  length, delta matched dipole at  $\lambda/4$  mounting height, shown in blue, against the pattern for the previously documented single wire cut-delta quad with two  $\lambda/2$  arms, shown in red. Lack of radiation off the ends of the simple dipole becomes more marked as the elevation angle becomes less. For comparison, the pattern for an inverted "Vee" dipole with 90° included angle and apex at 13.5 metres, corresponding to an average antenna height of 10 metres or  $\lambda/4$  approximately, is shown in green. Low elevation angle radiation performance is intermediate between the red and blue patterns. Figure 17 gives the simple dipole elevation patterns for azimuths of 0°, 45°, and 90°. See figure 20 for the configuration and wire coordinates.

## 11. Inverted Vee $\lambda/2$ 'Dipole'

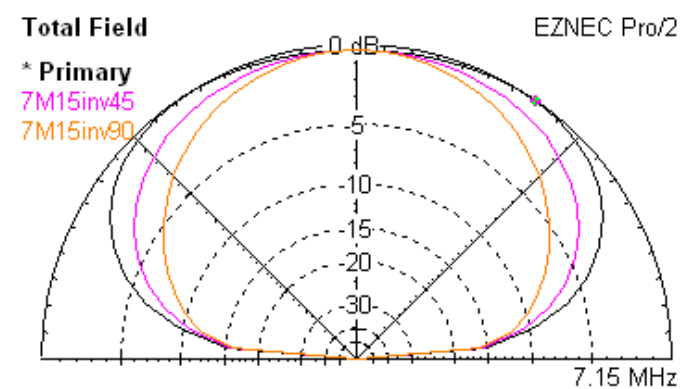


Fig 18: Elevation Patterns Inverted Vee, Az. 0°, 45°, 90°

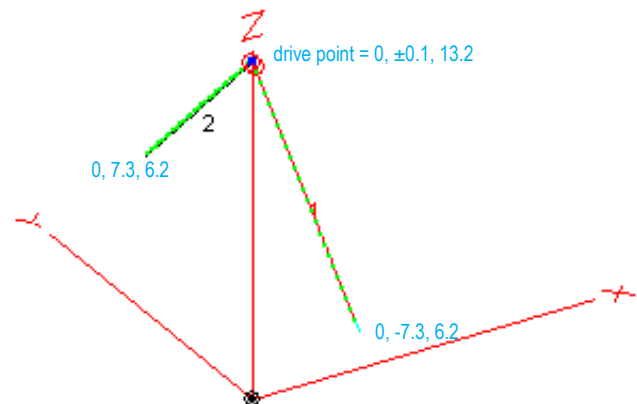


Fig 19 : Inverted Vee  $\lambda/2$  'Dipole'

Figure 18 shows elevation patterns for an inverted Vee of fig. 19 with two  $\lambda/4$  arms of 90° included angle, total length  $\lambda/2$ , driven at the apex of the inverted Vee at height 13.2 metres above soil of conductivity 10 mS/m and dielectric constant 13. Azimuth = 0° is the plane at right angles to the plane containing the Vee, azimuth = 90° is the plane containing the Vee.

<sup>7</sup> inclusion based on a suggestion by Owen Duffy, VK1OD, with the comment that the omni-directionality requirement for 90° phase difference between adjacent arms of a turnstile antenna is on occasion overlooked by antenna constructors.

Whilst directionality is greater than for the turnstile or cut-delta with  $\lambda/2$  arms, the approach to a quasi-omnidirectional antenna is much better than for the simple horizontal dipole. Performance in terms of lack of directivity is good for such a simple configuration. Additional benefits are the possibility of using only a single support mast, and the drive point impedance  $\approx 55 \Omega$  resistive, giving a good match to  $50 \Omega$  cable via a simple 1 : 1 balun, which may be either double wound or a Guanella type mounted on the mast. Zenith gain = 4.7 dBi, maximum gain = 5.0 dBi @  $60^\circ$  elevation. Interestingly, if the Vee is tilted back into the horizontal plane at a height of 10 metres, to form a simple half wave dipole distorted into a  $90^\circ$  Vee or short quadrant, then the peak gain increases slightly while the pattern shape remains virtually unchanged. Drive point impedance now is  $\approx 48 \Omega$  at resonance. Three elevated suspension points are now required.

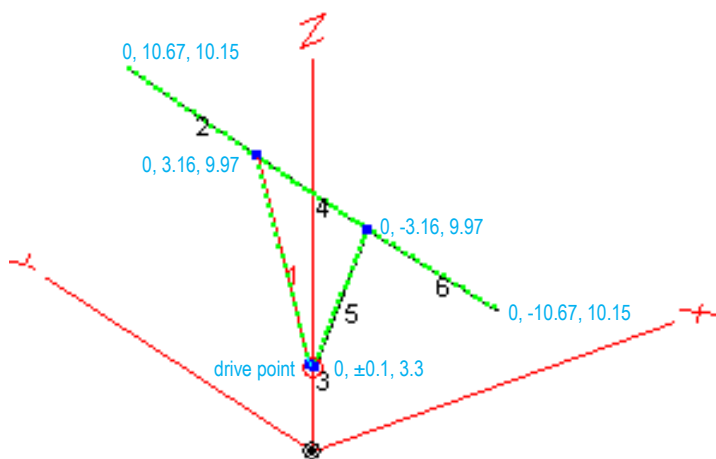


Fig 20 : Simple  $\lambda/2$  Delta Matched Dipole @  $\lambda/4$  height

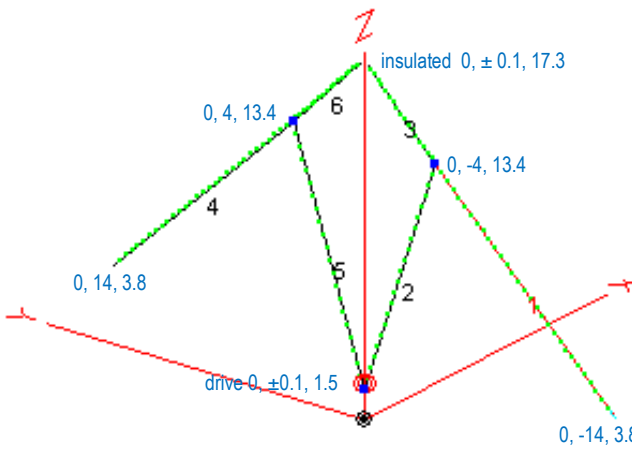


Fig 21 : Inverted Vee Cut Delta Quadrant with  $\lambda/2$  Arms

## 12. Inverted Vee Cut-Delta Quadrant

Figures 22 and 23 show the elevation and azimuth patterns for an inverted Vee cut-delta quadrant with  $\lambda/2$  arms and a  $90^\circ$  included angle between the arms, i.e. the previously horizontal quadrant has been tilted  $90^\circ$  to now lie in a vertical plane. Configuration, shown in fig. 21, is a cut-delta quadrant with the aspect of an inverted Vee antenna. Apex of the Vee is at 17.3 metres height, outer arms at 3.8 metres height, drive point of the delta match at 1.5 metres height, tap points at 5.46 metres from the 'cut' at the apex, soil parameters = conductivity 0.01 mS/m,  $\epsilon = 13$ . Azimuth =  $0^\circ$  is the X-Z plane of the Vee. Pattern is essentially circular at  $20^\circ$  elevation and also at angles approaching the zenith. Departure from omnidirectionality is a modest  $\pm 2$  dB at  $45^\circ$  elevation, while low angle radiation has improved significantly. Gain at the zenith is now only 3.1 dBi, traded off for the improved gain at low elevations. Only a single support mast is required, but height has now increased to 17.3 metres. Drive point impedance  $\approx 600 \Omega$ . Bandwidth for VSWR  $\leq 2$  is 6.85 – 7.45 MHz.

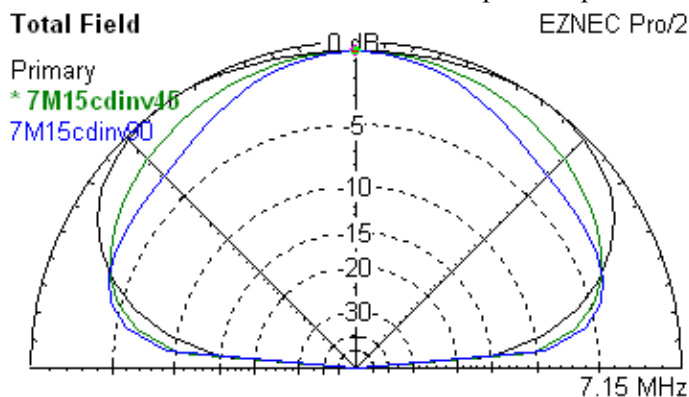


Fig 22 : Elevn. Cut-Delta Inv. Vee @ Az  $0^\circ$ ,  $45^\circ$ ,  $90^\circ$

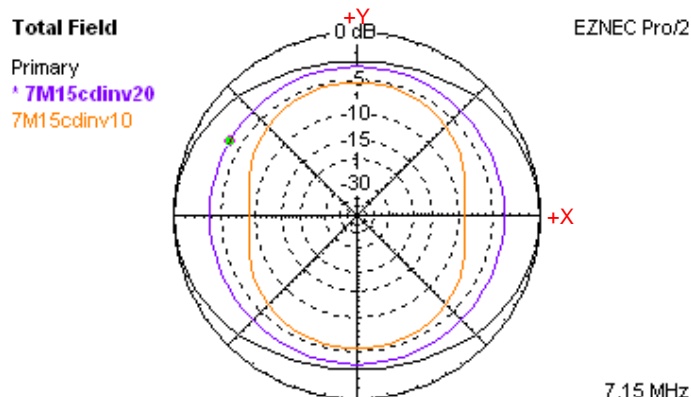


Fig 23: Azmth Cut-Delta Inv. Vee @ El.  $45^\circ$ ,  $20^\circ$ ,  $10^\circ$

### 13. Inverted Vee Turnstile

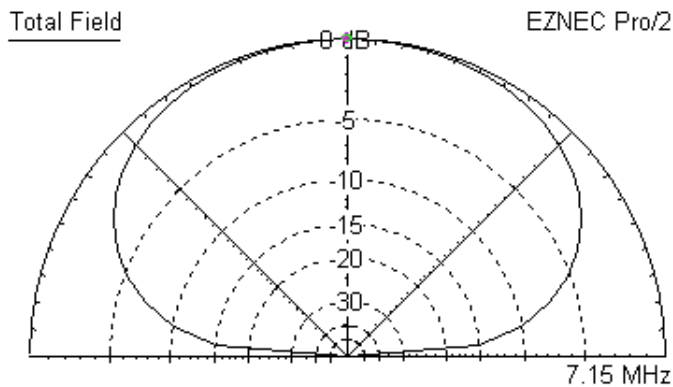


Fig 24 : Inverted Vee Turnstile Max. Gain = 4.9 dBi

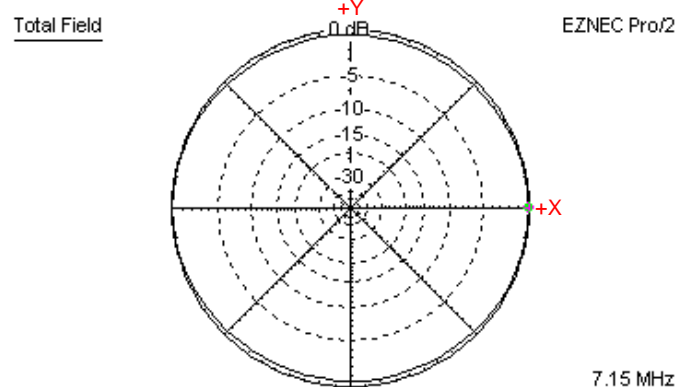


Fig 25 : Inverted Vee Turnstile @ 20° Elevn.

Figures 24 and 25 are the plots for two inverted Vees in turnstile configuration with a common drive point. Configuration and wire coordinates are shown in figure 27. Maximum gain = 4.9 dBi towards the zenith with circular polarisation. Azimuth pattern is omnidirectional  $\pm 0.25$  dB. To obtain the correct phasing, length of the +ve Y arm is 10.68 m, length of the -ve X arm is 9.97 m, with the apex of the +ve Y and X arms connected together at a height of 13.5 metres. Drive point impedance  $\approx 53 \Omega$ .

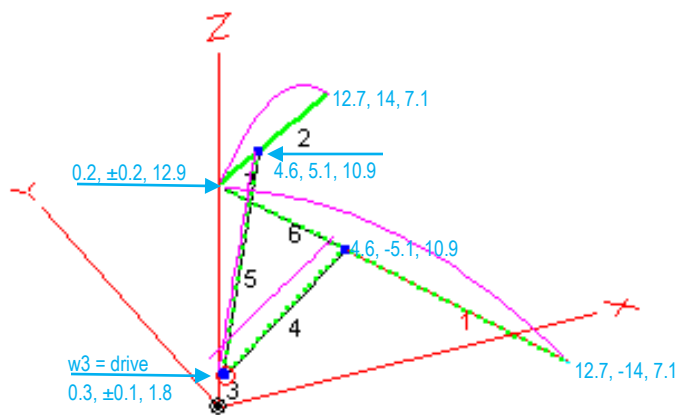


Fig 26 : Tilted 25° Cut-Delta Quadrant 3-D with Co-ords.

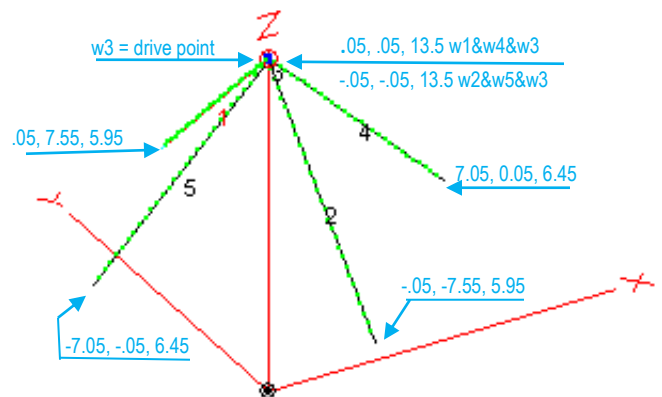


Fig 27 : Inverted Vee Turnstile 3-D with Co-ords.

### 14. Tilted Cut-Delta Quadrant

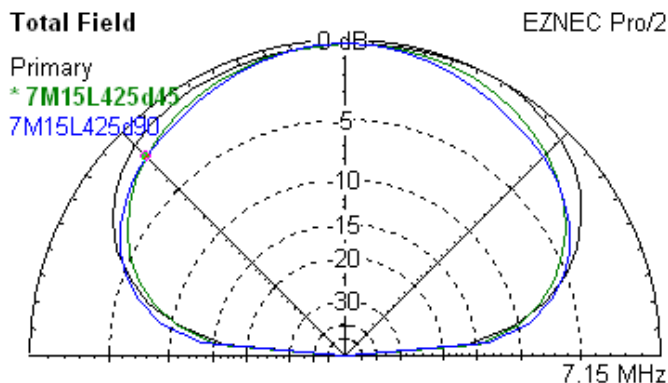


Fig 28 : Elevation Patterns Tilted Cut-Delta 0°, 45°, 90° Az.

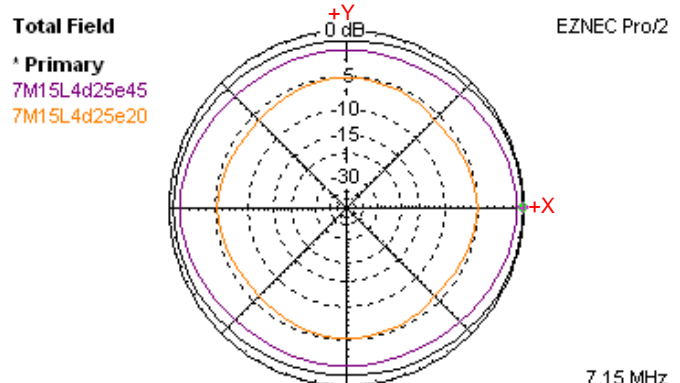


Fig 29 : Azimuth Patterns Tilted Cut-Delta 65°, 45°, 20° El.

Figures 28 and 29 are the elevation and azimuth patterns respectively for a cut-delta quadrant with its apex at 13 metres. Plane of the radiating arms has been tilted downwards by  $25^\circ$  from the apex along the line of symmetry. Configuration is given in figure 26. This places the average height of the radiating arms at 10 metres and the height of the outer arms at 7 metres, allowing use of a single main mast plus outhauls to ground level, or to stub poles of height 2 – 3 metres to save space. Maximum gain is 5.2 dB at  $65^\circ$  elevation along the axis of symmetry for a vertical mirroring plane. Patterns differ in minor respects from the horizontal cut-delta quadrant at  $\lambda/4$  mounting height.

## 15. Wells Cage Quadrant

Pattern of a Wells Quadrant at  $\lambda/4$  suspension height with a 5-wire cage of 2.8 mm. diameter copper wires is shown in figures 30 and 31. Spreaders are a symmetrical "X" shape using 1 metre diagonals, with 4 wires forming the outside of the cage and the 5th. wire central along the cage arm axis of symmetry. Calculated for ground of  $\sigma = 5 \text{ mS/m}$ ,  $\epsilon = 13$ .

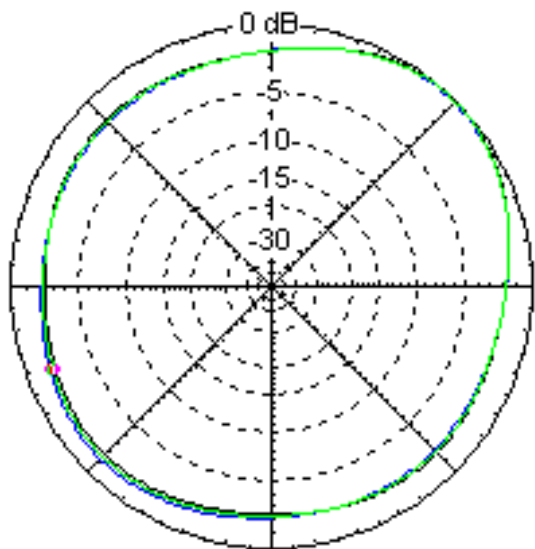
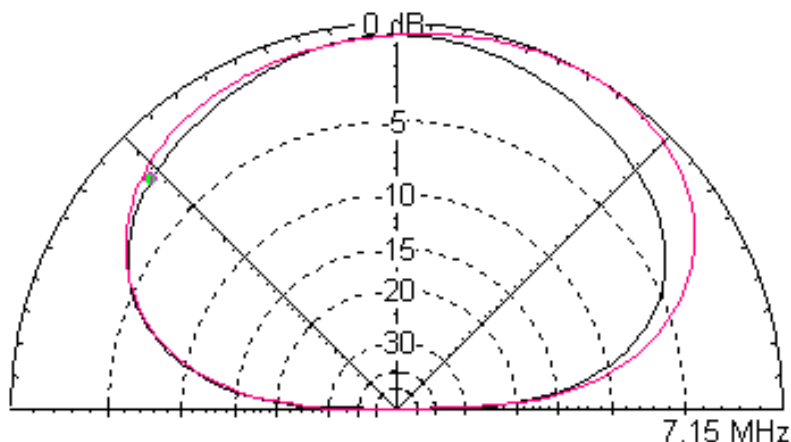


Fig. 30 : Azimuth @  $45^\circ$  Elvn. 6.9, 7.15, 7.4 MHz Fig



31 : Elevation Patterns Along Symtry.Axis,  $90^\circ$  to Axis

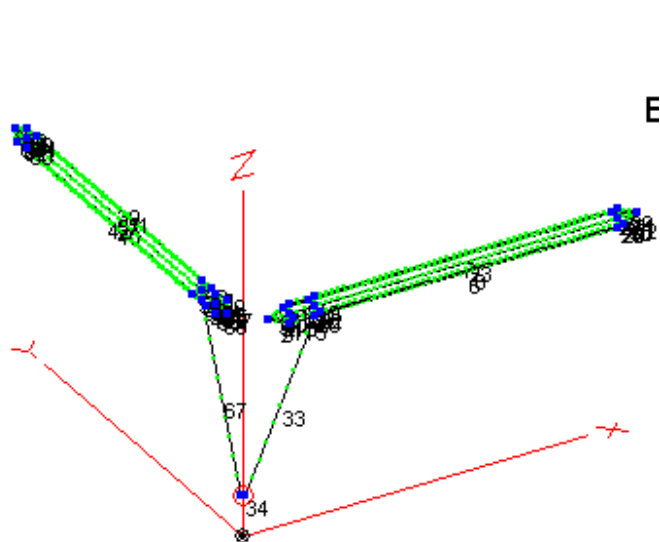


Fig 32 : Basic Antenna Layout :

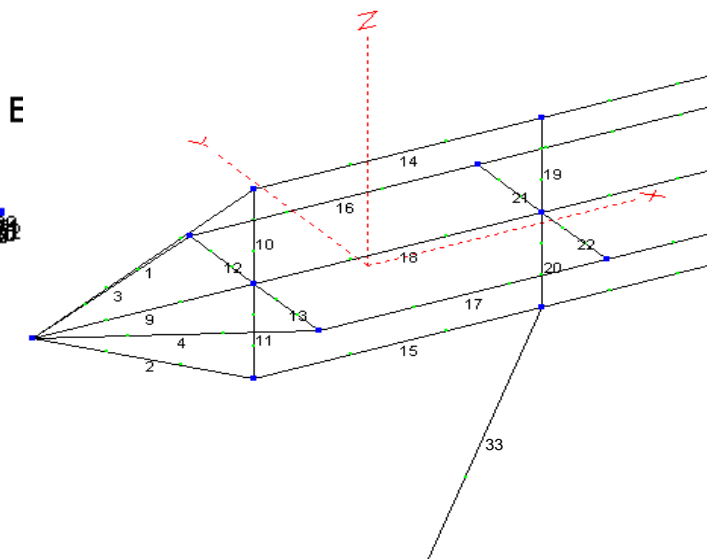


Fig 33 : Detail at Drive Point of Arm on X-axis :

At band centre of 7.15 MHz maximum gain was 6.0 dBi at 60° elevation along the axis of symmetry for the quadrant with impedance =  $608 + j\ 4\ \Omega$ . Using stainless steel wire rope reduced the gain by 0.5 dB with impedance now =  $650 + j37\ \Omega$ . (Stainless steel wire rope may present high resistance joints with nonlinearities unless silver brazing alloy is employed.) Axis of quadrant symmetry is midway between X and Y axes. Antenna drive point on Fig. 32 is red circled wire no. 34 of length = 200 mm. and height above ground = 2 metres. I.e. lower ends of wires 33 & 67 are separated by 200 mm.

In figure 33 note that "wires" 10 – 13 inclusive constitute a cage spreader : an 'X' shaped assembly typically fabricated from 12 or 19 mm. tubing. Wires 9, 18 etc. are the centre wires of the 5 wire cage. Lighter gauge intermediate spreaders are customarily employed. To save weight these may be insulating low-loss plastic tube or rod such as black delrin at 3 or 4 metre intervals.

MHz	Impedance	600 $\Omega$ VSWR	MHz	Impedance	600 $\Omega$ VSWR
6.67	$793 - j\ 451$	2.01	7.20	$601 + j\ 46$	1.08
6.90	$673 - j\ 219$	1.44	7.25	$595 + j\ 89$	1.16
6.95	$656 - j\ 172$	1.33	7.30	$591 + j\ 131$	1.25
7.00	$641 - j\ 127$	1.24	7.35	$589 + j\ 172$	1.34
7.05	$628 - j\ 83$	1.15	7.4	$587 + j\ 214$	1.43
7.10	$617 - j\ 39$	1.07	7.65	$602 + j\ 425$	2.00
7.15	$608 + j\ 4$	1.015			

Table 6 : Drive Point Impedance and VSWR vs. Frequency for 7.15 MHz Wells Cage Quadrant

Table 6 is the drive point impedance for the antenna after cage dimensions, including arm lengths and arm tapping point, have been optimised for resonant frequency, antenna mounting height and ground parameters. The entire 7.0 – 7.3 MHz amateur band has been covered with  $VSWR \leq 1.25$ .

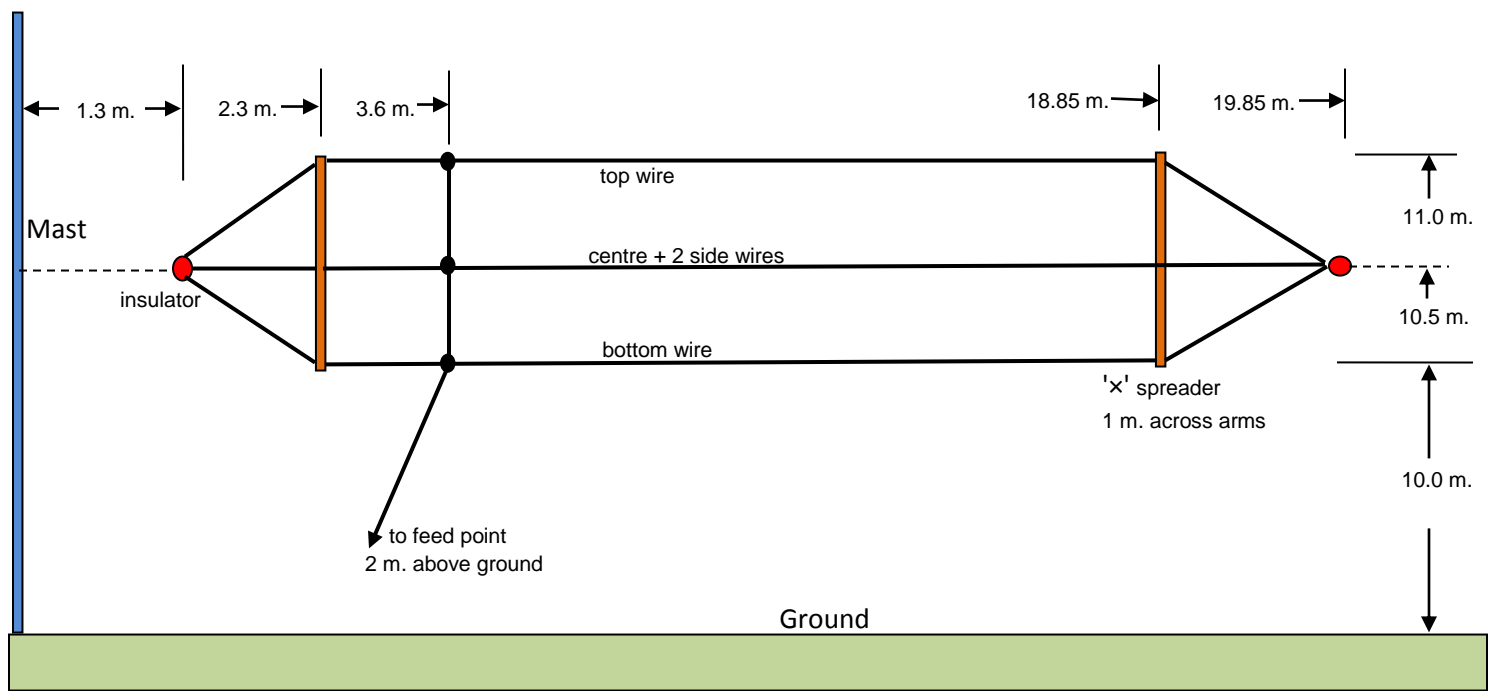


Fig 34 : Dimensions of One Arm of Cage Quadrant : Not to scale.

### 16. Stacked Wells Cage Quadrant

If cage quadrants are stacked or tiered at heights above ground of  $\lambda/2$  and  $\lambda$ , and driven in-phase at the apex of each quadrant, then low takeoff angle radiation is enhanced and the high angle lobe is virtually eliminated. This is a useful

configuration for commercial use at the upper end of the shortwave band, at frequencies where high angle radiation would be wasted by simply penetrating the ionosphere to disappear into space. A quasi-omnidirectional azimuth pattern having significant effective power gain at low takeoff angles can be produced.

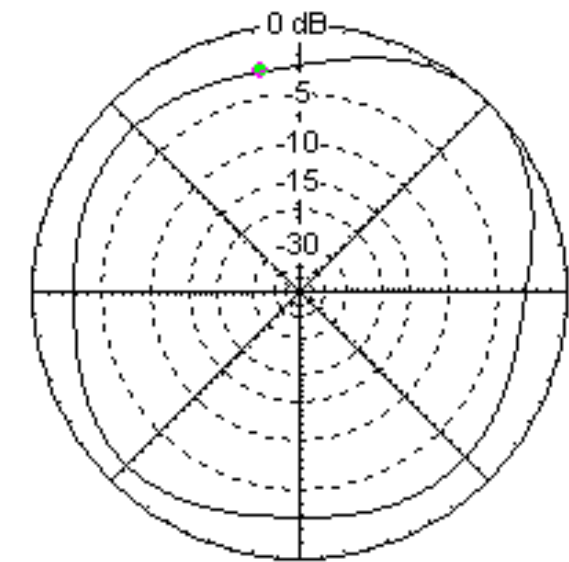


Fig 35 : Azimuth Pattern for Stacked Cage Quad

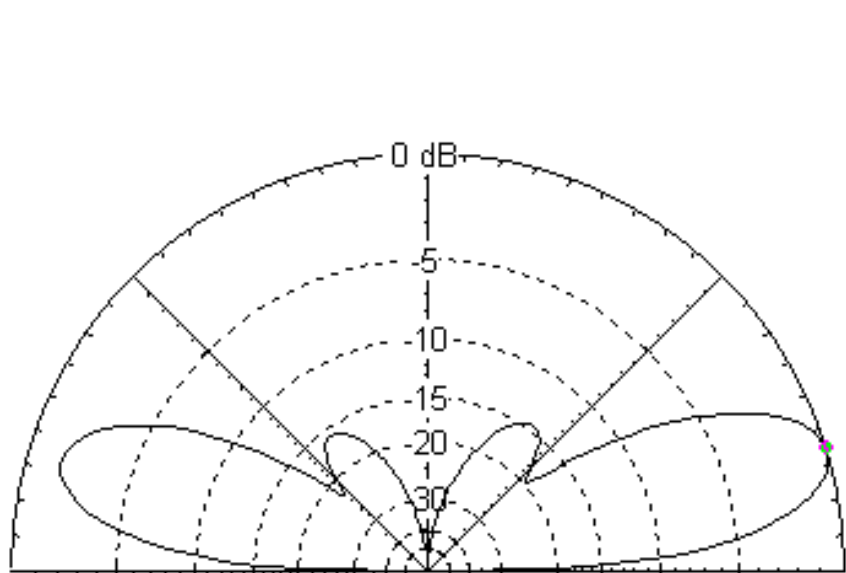


Fig 36 : Elevation Pattern for Stacked Cage Quad

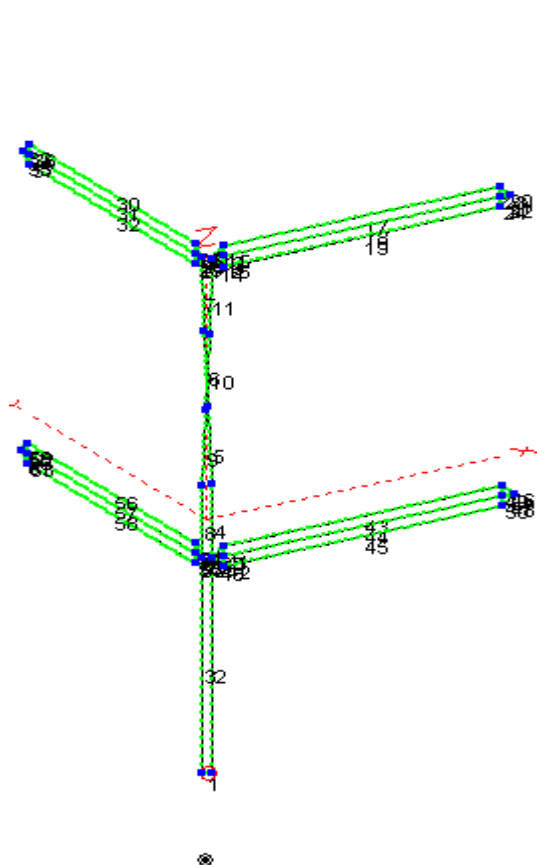


Fig. 37 : Perspective View of Stacked Quadrant

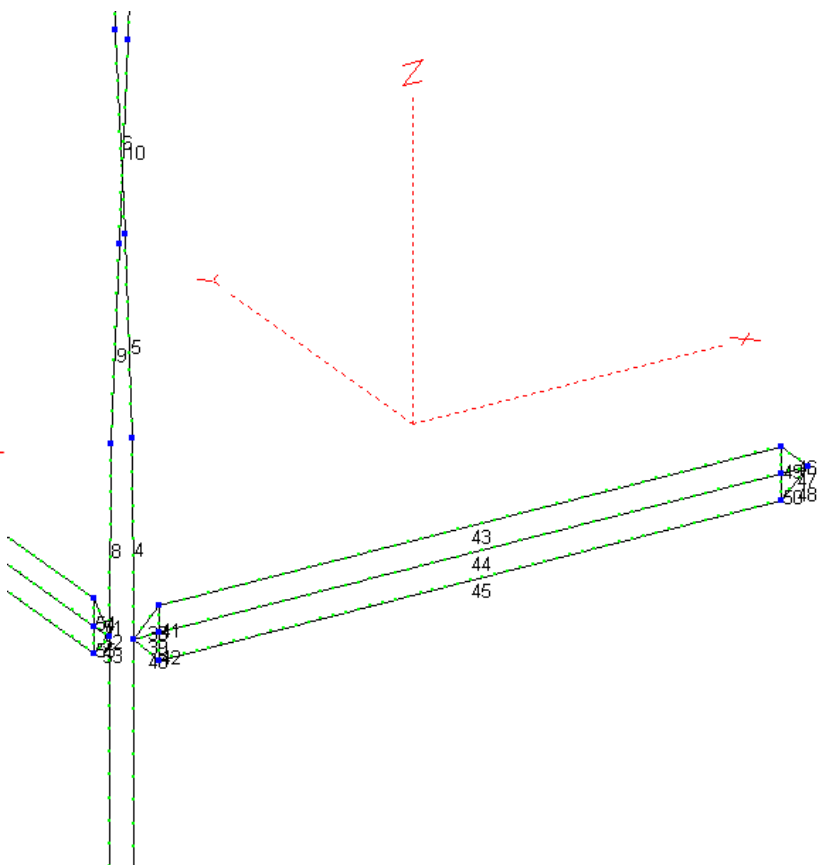


Fig. 38 : Detail of Lower Cage Quadrant and Feeders.

Each cage has been reduced to a flat grid of 3 wires separated by straight spreaders. This produces a drive point impedance of 1200  $\Omega$  for each quadrant after allowing for interaction between the two quadrants and their two images in

the ground. The quadrants have then been interconnected by an  $\lambda/2$  transmission line, effectively placing the two quadrant drive point impedances in parallel at the drive point of the lower quadrant since impedances repeat at  $\lambda/2$  intervals along a transmission line. The interconnecting  $\lambda/2$  line between the two quadrants must have a  $180^\circ$  twist to ensure correct phasing of the two drive points since there is a further  $180^\circ$  phase delay attributable to propagation along the line. Usually a minimum of 3 intermediate spacers are used on this line. Fig. 35 shows the azimuth plot at  $17^\circ$  takeoff angle for a stacked cage of this type at 21.225 MHz. Maximum gain is 9.6 dBi, front to sidelobe ratio 1.5 dB, minimum gain 6.5 dBi at azimuths of  $100^\circ$  and  $350^\circ$  (green dot is at  $100^\circ$  azimuth). Fig. 36 is the elevation plot along the axis of symmetry at  $45^\circ$  azimuth. Maximum gain is 9.6 dBi at  $17^\circ$  takeoff angle with a -3dB beamwidth at  $8^\circ$  and  $27^\circ$  elevation angles.

Figure 37 shows a perspective view of the antenna, while Fig. 38 is a detail of the throat and feeder attachments to the lower quadrant arms. Note again the  $180^\circ$  twist or crossover for the feeder between the lower and upper quadrant. All wires were 2.8 mm. hard drawn copper wire (also known as "200 lb. per mile H.D.copper" : # 9 AWG/B&S or # 11 SWG or #12 Stubs' Birmingham gauge are close ) Feeder wire spacing was 200 mm. with the bottom feed point terminating at 2 metres above ground to allow for a pole mounted balun transformer<sup>8</sup>. Insulating stays or ropes should be attached to each grid (or degenerate 'cage') to prevent rotation with consequent "windup" leading to premature antenna failure.

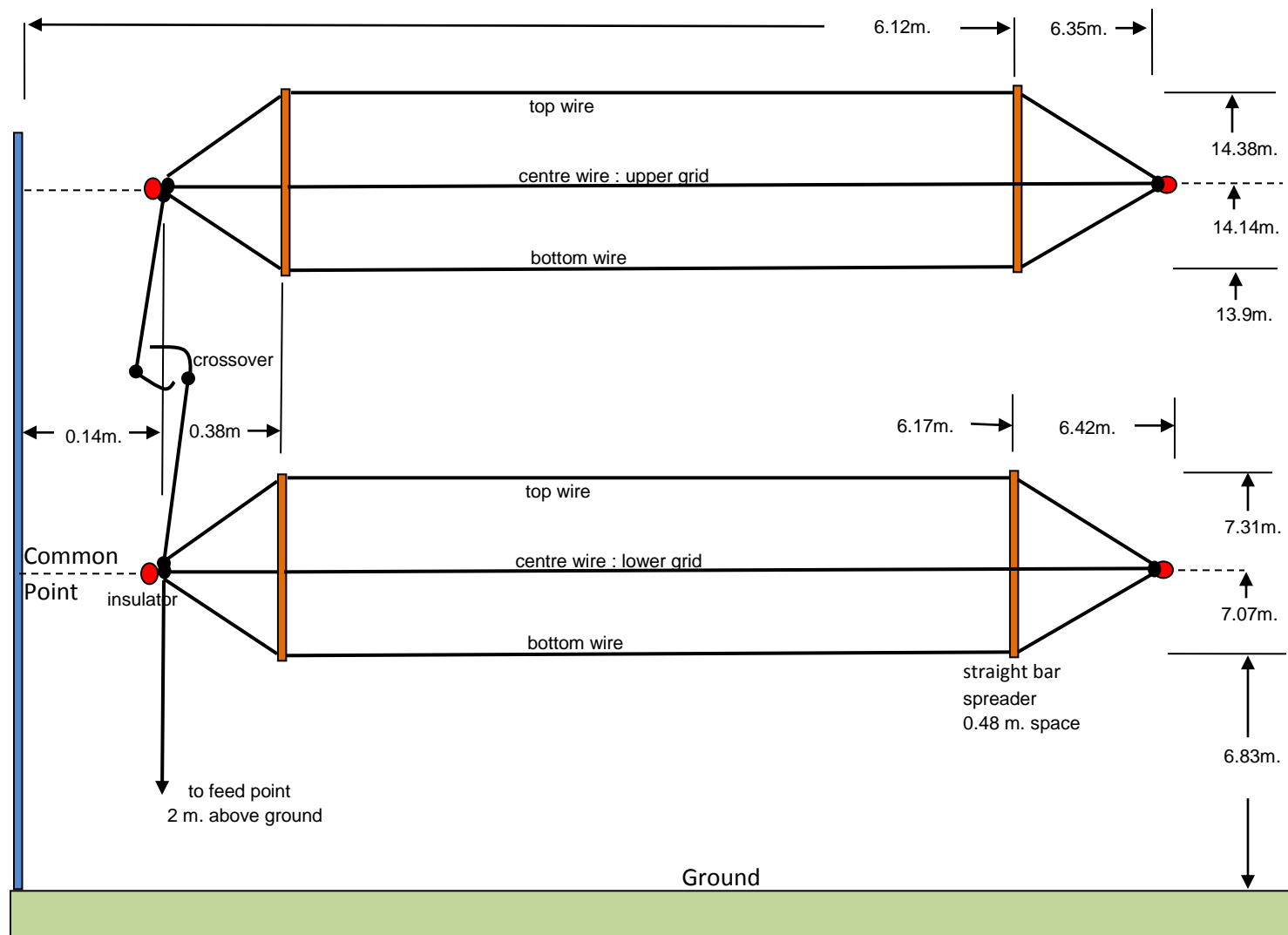


Fig. 39 : Dimensions of Upper and Lower Tiers of Quadrants

<sup>8</sup> more ground clearance may be required depending on power level and requirements for security from inadvertent access



Frequency MHz	Impedance $\Omega$	VSWR 600 $\Omega$	Frequency MHz	Impedance	VSWR 600 $\Omega$
20.00	360 – j 239	2.04	21.225	586 – j 28	1.05
20.25	386 – j 187	1.79	21.25	594 – j 26	1.05
20.50	420 – j 137	1.56	21.30	610 – j 22	1.04
20.75	464 – j 92	1.36	21.35	627 – j 19	1.06
21.00	522 – j 53	1.18	21.40	645 – j 17	1.08
21.05	535 – j 47	1.15	21.45	663 – j 17	1.10
21.10	549 – j 40	1.12	21.75	784 – j 38	1.31
21.15	563 – j 35	1.09	22.00	889 – j 103	1.52
21.20	578 – j 30	1.07	22.25	972 – j 222	1.75
			22.50	1000 – j 384	2.02

Table 7 : Drive Point Impedance and VSWR vs. Frequency for 21.225 MHz Stacked Wells Cage Quadrant

Figure 39 gives the dimensions of the 21.225 MHz Stacked Wells "Cage" Quadrant while Table 7 gives the drive point impedance 2 metres above 'average' ground for the antenna. Arm lengths differ slightly between the upper and lower arms since the method of synthesis was to initially adjust the arm length of each tier independently for near equality of drive point impedance  $\approx 1200 \Omega$  resistive at band centre, noting that impedance is a function of interaction between tiers and also with the images in the ground. Feeders were then added to the calculation and the antenna dimensions subjected to further fine adjustment to optimise drive point impedance.

## 17. Two Stacked Single Wire Stacked Quadrants @ 21.225 MHz

Figures 40 and 41 are the azimuth pattern at  $17^\circ$  elevation and elevation pattern at  $45^\circ$  azimuth respectively for two single wire quadrants stacked at  $\lambda/2$  and  $\lambda$  height above average ground at 21.225 MHz. Maximum gain is 8.4 dBi and the -3 dB points for elevation pattern are at  $8^\circ$  and  $27^\circ$ . Matching to 600  $\Omega$  uses a stub with the feed 1.08 m above the short circuit..

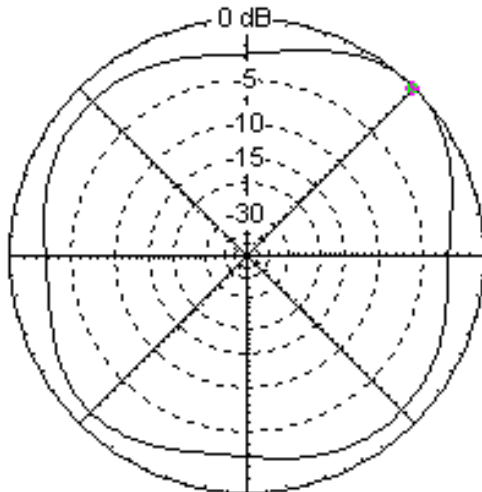


Fig. 40 : Azimuth Pattern 2 x sw. Quads

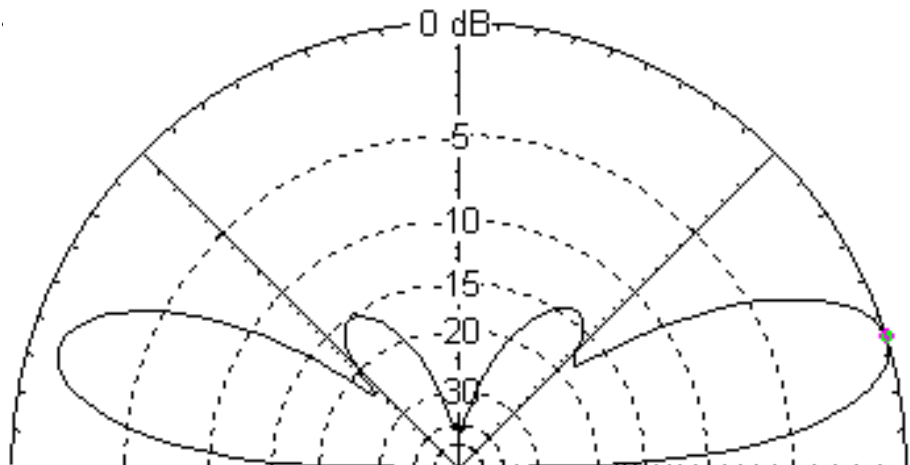


Fig 41 : Elevation Pattern of two single wire stacked quadrants : stub match

Frequency MHz	Impedance $\Omega$	VSWR rel. 600 $\Omega$	Frequency MHz	Impedance $\Omega$	VSWR rel. 600 $\Omega$
20.825	709 + j 441	1.98	21.30	528 – J 46	1.16
21.00	739 + j 214	1.46	21.40	446 – J 70	1.39
21.10	692 + J 94	1.23	21.45	408 – J 73	1.51
21.225	594 – J 9	1.02	21.60	313 – J 66	1.95

Table 8 : Drive Point Impedance of two stacked single wire quadrants with stub match

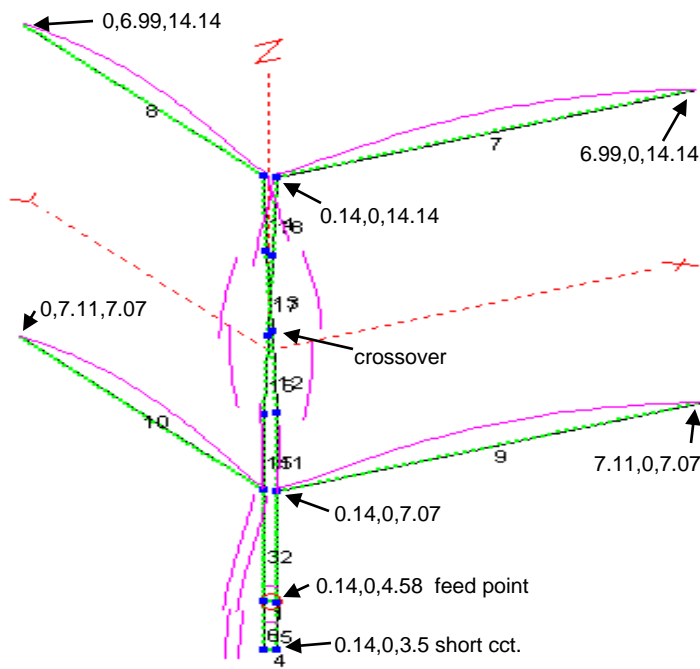


Fig 42 : stacked single wire quadrants : stub match.

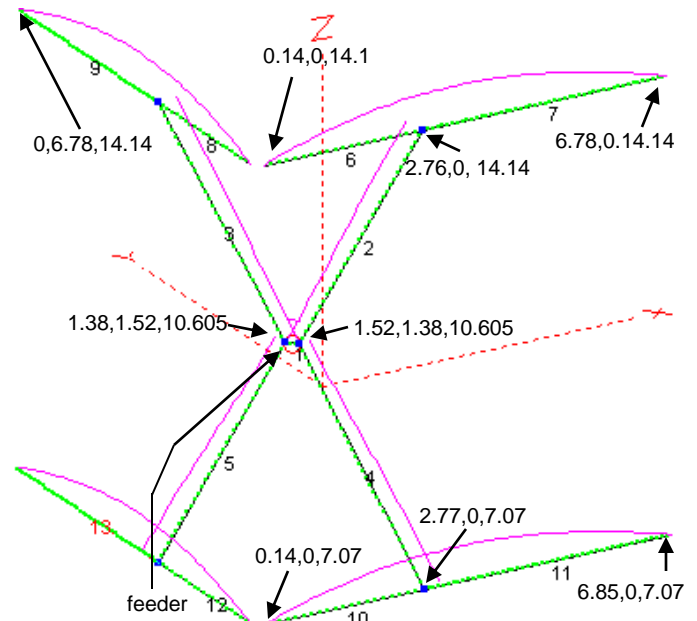


Fig 43 : stacked single wire quadrants : tapped match

Figure 42 shows the general configuration for the two stacked single wire quadrants using a  $600\ \Omega$  feeder with a tapped shorted stub match. The feed to the upper level requires a crossover. Figure 43 is an alternative arrangement where each quadrant is treated as a separate cut delta matched quadrant configured as a  $1200\ \Omega$  match at the feed point after interaction between the two antennas and the ground is taken into account. The lower delta has been inverted to create a common feed point of  $600\ \Omega$  impedance for the overall array. No crossover is required as the central feed point ensures that both sections of the array are in phase. Purple lines show the magnitude of the current in each wire. For the cut delta match the current in each delta arm is almost constant in magnitude but undergoes a significant progressive phase change with distance. In the radiating arms of the quadrant, current is zero at the ends, maximum at the centre, with a step change of phase, but little change in magnitude, at the point where the delta match wire connects to the radiating arm. This appears to be close to the optimum matching and bandwidth condition for the single wire cut-delta quadrant. All dimensions are in metres on an X-Y-Z three dimensional co-ordinate system

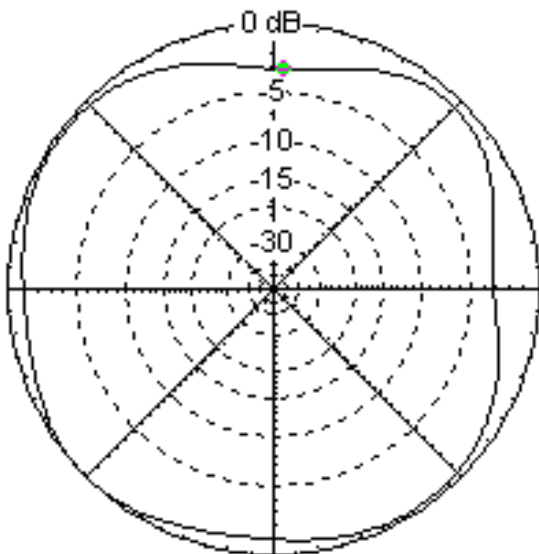


Fig. 44 : Azimuth 2xsw.Qd. : Tapped Match

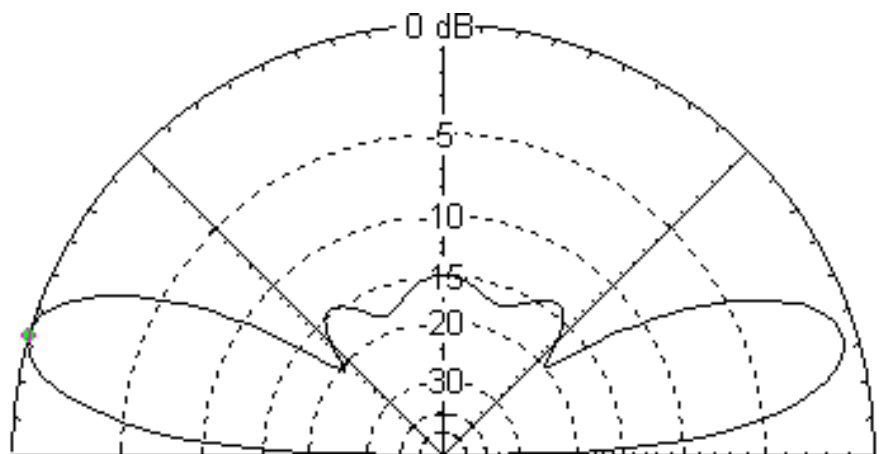


Fig. 45 : Elevation Pattern : 2 single wire quadrants : Tapped Match

Note that the feeders would normally be initially routed in a direction perpendicular to the stub matched feeder or perpendicular to the plane of the delta arms of the cut delta match until well clear of the antenna. A typical route for the feeder is shown in figure 43.

Table 9 has the drive point impedance and VSWR relative to 600  $\Omega$  versus frequency for the two-stack cut-delta quadrant antenna. Bandwidth of the antenna is better than for the stub matched case, however the feeder and matching arrangements are more complex. Radiation from the delta match sections has caused the pattern at 225° azimuth to exceed the radiation at 45° azimuth for this configuration.

Frequency MHz	Impedance $\Omega$	VSWR rel. 600 $\Omega$	Frequency MHz	Impedance $\Omega$	VSWR rel. 600 $\Omega$
20.325	634 – j 437	2.01	21.30	640 + j 30	1.086
21.00	594 – j 124	1.23	21.40	668 + j 86	1.19
21.10	604 – j 74	1.13	21.45	684 + j 114	1.25
21.225	624 – j 9	1.04	21.90	967 + j 394	2.00

Table 9 : Drive Point Impedance and VSWR vs. Frequency for Two-Tier Cut-Delta Quadrant

Other matching systems for the stacked or tiered single wire quadrants are possible. However the tempting expedient of a single cut-delta match to the lower quadrant, combined with an  $\lambda/2$  twisted crossover 600  $\Omega$  line to connect the 'throats' of the upper and lower quadrants does not produce a good pattern. Current flow towards the 'throat' from the delta attachment points, to provide power to the upper quadrant, significantly disrupts the radiation pattern.

## 18. Antenna Orientation

For the simple dipole and inverted Vee types, where the entire antenna can be contained in a single vertical plane, preferred orientation is usually for that plane to be oriented in a north-south direction. This is equivalent to the Y-axis for all of the antenna configuration diagrams to be a north-south axis. For the horizontal cut-delta quadrant, also for the 25° tilted version and the simple dipole bent into a quadrant, the axis of symmetry for all configurations should preferably be in an east-west direction. Differences are only modest for other orientations.

Circularly polarised cases have been previously covered in the text.

## 19. Practical Considerations

Preceding information has been mostly based on theoretical calculations, using one of the many commercially available implementations of Numeric Electromagnetic Code (NEC). Practical experience over many decades has confirmed that this is a reliable guide to results achieved in practice, but small corrections are necessary to adjust to the real world.

In practice wires inevitably have a small amount of sag, forming a catenary, or hyperbolic cosine (  $z = \cosh x$  ) shape. Small discontinuities in wire slope occur at junctions and tapping points. These effects are usually secondary so no attempt has been made to include them in this simple comparison of antenna types.

"Average ground" was used in the calculations. Real ground constants may differ considerably from these assumptions at some sites, and may also display significant seasonal variations.

Insulators may add small parasitic capacitances and wire lengths depending on design and method of wire attachment. Encroaching objects such as masts, other antennas and structures may also produce a parasitic loading effect.

In most cases the erection of one or two trial antennas, with careful measurements of impedance versus frequency, will serve to quantify these effects and provide sufficient guidance to the necessary corrections to align theory with a real world site. Necessity for accurate impedance measurements may impose some difficulty as good RF impedance or admittance bridges are rare and treasured items, while even the simpler "home brew" R-X noise bridges may be difficult to calibrate and interpret. Results from simple return loss bridges with a fixed reference resistance are even harder to interpret.

## 20. Conclusions

- .1 Single wire "cut-delta quadrant" antennas can provide quasi-omni-directional coverage in azimuth from an antenna that is light and simple enough for amateur use.
- .2 A major disadvantage of the quadrant is the requirement for three suspension points in a right-angled triangular plan configuration. A balun transformer is also required.
- .3 Bandwidth of the single wire cut-delta quadrant is small compared to the original Wells cage quadrant, but adequate for amateur band consideration.
- .4 A wide range of drive point impedances can be achieved by appropriate choice of tap points and/or matching  $\lambda/4$  sections. A 600  $\Omega$  driving point impedance is convenient if a long feeder run is required as 600  $\Omega$  open-wire feeder has low loss compared to coaxial cable.
- .5 Some experimentation is likely to be required to allow for construction methods, insulator types, crimps or junctions, ground conductivity and dielectric constant etc. Also note that some of the calculations for drive point impedance were based on expediency rather than precise modeling of drive point geometry, so further fine adjustment is usually required for practical cases.
- .6 Single wire cut-delta quadrants have a much greater range of variables, dimensions, or design degrees of freedom than a simple dipole, making design and adjustment considerably more complex. Cage quadrants and stacked or tiered quadrants further increase the degrees of freedom, often making such designs a daunting task.
- .7 The single wire cut-delta quadrant is only one of many methods examined and compared for achieving a quasi-omni-directional azimuth pattern. If simplicity, space limitations, use of only a single support mast, and approximate omni-directionality are the main criteria then the simple inverted Vee 'dipole' may be the best option as the drive point impedance can provide a good match to 50  $\Omega$  coaxial cable with a simple 1 : 1 balun.
- .8 No attempt has been made in this simple comparison of antenna types to include loaded antenna types. Resistive, simple reactive, resonant trap antenna loading, or combinations of these, all add further degrees of freedom for design, with consequent tradeoffs. Some of these have been covered in a wide range of technical literature stretching back more than 2/3 of a century.

Ross Beaumont

VK2KRB

ver. 2 : 1nov'13 : figs. 14 & 15 plus commentary inserted.

ver. 3 : 8apr'15 : typical Wells cage quadrant dimensions & performance added, also a stacked wire quadrants, cage and single wire.